

# DispaRisk: Assessing and Interpreting Disparity Risks in Datasets\*

Jonathan Vasquez<sup>1,2</sup>, Carlotta Domeniconi<sup>1</sup> and Huzefa Rangwala<sup>1</sup>

<sup>1</sup>George Mason University

<sup>2</sup>Universidad de Valparaíso

{jvasqu6,cdomenic,rangwala}@gmu.edu, jonathan.vasquez@uv.cl

## Abstract

Machine Learning algorithms (ML) impact virtually every aspect of human lives and have found use across diverse sectors, including healthcare, finance, and education. Often, ML algorithms have been found to exacerbate societal biases presented in datasets, leading to adversarial impacts on subsets/groups of individuals, in many cases minority groups. To effectively mitigate these untoward effects, it is crucial that disparities/biases are identified and assessed early in a ML pipeline. This proactive approach facilitates timely interventions to prevent bias amplification and reduce complexity at later stages of model development. In this paper, we introduce **DispaRisk**, a novel framework designed to proactively assess the potential risks of disparities in datasets during the initial stages of the ML pipeline. We evaluate **DispaRisk**'s effectiveness by benchmarking it with commonly used datasets in fairness research. Our findings demonstrate the capabilities of **DispaRisk** to identify datasets with a high-risk of discrimination, model families prone to biases, and characteristics that heighten discrimination susceptibility in a ML pipeline. The code for our experiments is available in the following repository: <https://github.com/jovasque156/disparisk>

## 1 Introduction

Extensive research on fairness in machine learning (ML) has shown that algorithms can exacerbate historical and societal biases when trained on unchecked/biased datasets. This leads to harmful effects on minorities and disadvantaged groups [Pessach and Shmueli, 2023; Kizilcec and Lee, 2022; Wen *et al.*, 2021; Fu *et al.*, 2021], e.g., in criminal justice [ProPublica, 2016], healthcare [Chen *et al.*, 2023], and education [Vasquez *et al.*, 2022]. Previous research emphasizes the importance of identifying and mitigating biases in the early stages of a ML pipeline [Feldman *et al.*, 2015; Hardt *et al.*, 2016]. One solution is to identify potential risks of discrimination via *pre-training metrics*, which can be computed directly from the data before they are used for training the model. Several metrics have been proposed [Hardt *et al.*, 2021] including Class Imbalance (CL), Conditional Demographic Disparity in Labels (CDDL), and Difference in positive proportions in observed labels (DPL), and Mutual Information (MI) between the sensitive attribute and the rest of the features, since [Gupta *et al.*, 2021] showed that group disparities are bounded by this estimate. However, these approaches

do not provide evaluations that consider the characteristics of downstream ML models in a given pipeline. This limitation makes it challenging to answer questions such as which type of model is more likely to produce disparate outcomes when applied on the assessed dataset.

Prior research involves training a diverse set of models, followed by the computation of *post-training metrics*. This approach, discussed by [Hardt *et al.*, 2021; Vasquez *et al.*, 2022], serve two main purposes: firstly, to identify any existing discrimination (e.g., through Demographic Parity (DP), Accuracy Difference (AD), and Equalized Odd (ODD)); and secondly, to generate explanations of disparate predictions (e.g., through KernelSHAP). Despite the utility of this strategy for the late steps of a ML pipeline, they are applicable only to specific trained models of the pipeline. Therefore, if the models are retrained, or their hyperparameters are altered, these metrics need to be recalculated.

Irrespective of the advancements made, we still lack assessment approaches that are insightful, specific for the early stages of a ML pipeline, and, as a critical need, to be less dependent on specific instances of trained models of the ML pipeline. This work addresses this gap by leveraging recent research on *usable information*—actionable information under statistical and computational limitations [Xu *et al.*, 2020; Ethayarajh *et al.*, 2022; Hewitt *et al.*, 2021]—, and introduces **DispaRisk**, a framework for detecting and interpreting disparity risks in datasets prior to their use in downstream ML workflows. Given a ML pipeline context, **DispaRisk**: (1) identifies datasets that are more likely to lead to disparate outcomes; (2) identifies *model families* prone to produce disparities; (3) generates insights about the features that leak information about sensitive attributes; and (4) identifies individuals at a high-risk of being discriminated.

## 2 Fairness in Algorithms

All subsequent discussions are based on the setting described in this section. For a given ML pipeline, let  $X, S, Y$  be random variables in  $\mathcal{X} \times \mathcal{S} \times \mathcal{Y}$  representing features of individuals, the sensitive attributes, and a target variable to be predicted by a mapping function  $f : X \mapsto Y$ , respectively. Also, let  $\mathcal{A}$  be an agent with access to a space of possible mapping functions, which is constrained by computational and statistical constraints. Additionally, we assume that  $\mathcal{A}$  has access to

\*Work in progress

samples  $(x_i, s_i, y_i) \in \mathcal{X} \times \mathcal{S} \times \mathcal{Y}$ , and that learns a mapping function  $f$  from a given dataset  $\mathcal{D} = \{(x_i, y_i)\}_{i=1}^n$ .

Given this setting, we now outline three common fairness notions that will be used in this study, and then explore the relationship of fairness with recent information theories.

## 2.1 Fairness Notions.

Fairness in algorithms is commonly certified through independence ( $f(X) \perp S$ ), separation ( $f(X) \perp S|Y$ ), or individual notions ( $f(x_i) \approx f(x_j) \quad \forall i, j \text{ s.t. } d(x_i, x_j) < \epsilon$ , with  $\epsilon > 0$  and  $d$  a distance function) [Feldman *et al.*, 2015; Hardt *et al.*, 2016; Pessach and Shmueli, 2023; Vasquez *et al.*, 2022]. [Pessach and Shmueli, 2023] provide a comprehensive survey of which we replicate the three most commonly used metrics:

**Definition 1** (Demographic Parity (DP)). *Demographic Parity evaluates the difference in the predictive positive rate across demographic groups:*

$$\Delta_{DP}(f, S) = \max_{s \in S, s' \in S} |P(f(X) = 1|S = s) - P(f(X) = 1|S = s')|$$

**Definition 2** (Equalized Odds (ODD)). *Equalized Odds measures the difference in the true and false positive rates across demographic groups:*

$$\Delta_{ODD}(f, S, Y) = \max_{s \in S, s' \in S} \frac{1}{2} \sum_{c \in \{0, 1\}} |P(f(X) = 1|S = s, Y = c) - P(f(X) = 1|S = s', Y = c)|$$

**Definition 3** (Equalized Opportunity (OPP)). *Equalized Opportunity is a weaker requirement of Equalized Odds, focusing only on the true positive rate:*

$$\Delta_{OPP}(f, S) = \max_{s \in S, s' \in S} |P(f(X) = 1|S = s, Y = 1) - P(f(X) = 1|S = s', Y = 1)|$$

## 2.2 Fairness Through Usable Information.

Mutual Information (MI) measures the reduction in uncertainty of one random variable due to the knowledge of another [Cover and Thomas, 2006]. It is formally defined as  $I(A; B) = H(A) - H(A|B)$ , where  $A$  and  $B$  are random variables, and  $H(\cdot)$  is the entropy. Previous studies leveraged MI to mitigate bias in datasets by learning a representation  $Z$  of the input space that minimizes the amount of information about the sensitive attribute  $S$  [Gitiaux and Rangwala, 2021; Gitiaux and Rangwala, 2022; Gupta *et al.*, 2021]. These approaches are substantiated by the theorem shown by [Gupta *et al.*, 2021], which demonstrates that for any mapping function  $f$  acting on  $Z$ , the respective DP is bounded by  $I(Z; S)$ . Consequently, any reduction in  $I(Z; S)$  will also decrease the disparity of  $f$  acting on  $Z$ . The underlying intuition is that the more information  $Z$  contains about  $S$ , the higher is the risk of disparate outcomes for any function  $f$  acting on  $Z$ . Based on this notion, one could assess a given dataset by estimating  $I(X; S)$ , and generate insights on risks of disparities by assessing whether a higher estimation of MI is obtained. However, while this evaluation approach is useful for identifying

the risk that **any** function  $f$  acting on  $X$  might pose, it does not allow to distinguish which specific type of function  $f$  is more likely to result in higher disparate outcomes, since the estimation of MI serves as an upper bound for all functions. To address this limitation, we propose to employ *usable information*, a concept that generalizes Shannon information formulated by [Xu *et al.*, 2020], whose underlying intuition *usable information* and formulation are described next.

*Usable information* intuitively suggests that different agents using the same dataset for a task can leverage a different amount of *information*, depending on their computational capabilities. Thus, from each agent's perspective, the dataset is a resource of a varying amount of *usable information*. For example, consider the case of a decryption task. Under Shannon information theory, the original and encrypted messages have high MI; thus, two different decrypters with unlimited computational capabilities should be able to obtain the original message. However, in practice, the assumption of unlimited computational resources is not met, and their success depends on how much *usable information* is in the encrypted message for each decrypter. Consider a second example where, for binary classification, one of the agents has access only to logistic regression mapping functions, while the second has access to mapping functions comprised by affine functions followed by softmax. Similar to the decryption task, by computing the *usable information* on the target variable for each agent, we can now assess which one is more prone to produce better predictions. Indeed, by adhering to the fundamental principle of the theorem of [Gupta *et al.*, 2021], we can compute the *usable information* on the sensitive attribute for each agent, and estimate which agent is at a higher risk of discriminating by using the corresponding family of mapping functions.

From [Xu *et al.*, 2020], the constraints of an agent are modeled as a *predictive family*  $\mathcal{V}$ , which represents a collection of predictive models an agent can use for their tasks. As such, a predictive family may be restricted for statistical constraints or computational limitations, and it must satisfy *optional ignorance*. For the formal definitions of these two, let  $\mathcal{P}(\mathcal{Y})$  represent the set of all probability measures on  $\mathcal{Y}$ , and  $\emptyset$  the absence of any *side information*. Side information refers to samples from a feature space. For instance, in toxicity analysis, a *side information* can be a text sampled from a corpus of tweets  $X$ , and  $\emptyset$  a post of zero characters. Given this, a predictive family is formally defined as [Xu *et al.*, 2020]:

**Definition 4** (Predictive Family). *A set  $\mathcal{V} \subseteq \Omega = \{f : \mathcal{X} \cup \emptyset \mapsto \mathcal{P}(\mathcal{Y})\}$  is a predictive family if it satisfies the optional ignorance condition:*

$$\begin{aligned} \forall f \in \mathcal{V}, \forall P \in \text{range}(f), \quad \exists f' \in \mathcal{V}, \\ \text{s.t. } \forall x \in \mathcal{X}, f'[x] = P, f'[\emptyset] = P \end{aligned}$$

where  $\text{range}(f)$  is the range of function  $f$ .

The *optional ignorance* condition captures the ability to disregard the side information when making predictions. For example, consider a predictive family built with linear regression functions. By setting certain parameters associated with a subset of features to 0, agent can *ignore* those features and generate predictions of the target variable  $Y$  within the set

$\mathcal{P}(\mathcal{Y})$ . The fulfillment of this condition is crucial to achieve desirable properties described at the end of this section.

We now reproduce the definition of predictive  $\mathcal{V}$ -information, also from [Xu *et al.*, 2020], which refers to the measure of the change in the predictability of variable  $Y$  when additional side information  $X$  is provided to a model in family  $\mathcal{V}$ . Formally:

**Definition 5** (Predictive  $\mathcal{V}$ -information). *Given the random variables  $X, Y$  taking values in  $\mathcal{X} \times \mathcal{Y}$  and the predictive family  $\mathcal{V} \subseteq \Omega = \{f : \mathcal{X} \cup \emptyset \mapsto \mathcal{P}(\mathcal{Y})\}$ , the predictive  $\mathcal{V}$ -information from  $X$  to  $Y$  is defined as:*

$$I_{\mathcal{V}}(X \mapsto Y) = H_{\mathcal{V}}(Y|\emptyset) - H_{\mathcal{V}}(Y|X)$$

where  $H_{\mathcal{V}}(\cdot)$  is the predictive  $\mathcal{V}$ -entropy:

$$H_{\mathcal{V}}(Y|X) = \inf_{f \in \mathcal{V}} \mathbb{E}_{x,y \sim X,Y} [-\log f[x](y)]$$

$$H_{\mathcal{V}}(Y|\emptyset) = \inf_{f \in \mathcal{V}} \mathbb{E}_{x,y \sim X,Y} [-\log f[\emptyset](y)]$$

with  $f[x] \in \mathcal{P}(\mathcal{Y})$  chosen for the given  $x$ ;  $f[\emptyset]$  implies that no side information is provided; and  $f[x](y)$  represents the density value evaluated at  $y \in \mathcal{Y}$ . The base of the log determines the units of information: 2 for **bits** and  $e$  for **nats**.

Finally,  $\mathcal{V}$ -information metrics satisfy the desirable properties listed below [Xu *et al.*, 2020]. From these properties, we can infer that if  $\mathcal{M} \subseteq \mathcal{V}$ , then  $I_{\mathcal{M}}(X \mapsto Y) \leq I_{\mathcal{V}}(X \mapsto Y)$ . Therefore, if  $\mathcal{V}$  is large enough to contain all possible models, i.e.  $\mathcal{V} = \Omega$ , the  $\mathcal{V}$ -information reduces to Shannon information.

1. **Non-Negativity:**  $I_{\mathcal{V}}(X \mapsto Y) \geq 0$ .
2. **Independence:** If  $X$  is independent of  $Y$ ,  $I_{\mathcal{V}}(X \mapsto Y) = I_{\mathcal{V}}(Y \mapsto X) = 0$ .
3. **Monotonicity:** If  $\mathcal{V} \subseteq \mathcal{U}$ , then  $H_{\mathcal{V}}(Y) \geq H_{\mathcal{U}}(Y)$ ,  $H_{\mathcal{V}}(Y|X) \geq H_{\mathcal{U}}(Y|X)$ .

Building on the theory discussed thus far, in the following section we present **DispaRisk**.

### 3 The DispaRisk Framework.

**DispaRisk** operates on two inputs: the sensitive attribute  $S$ , and the computational constraints  $\mathcal{V}$  of the downstream workflow.  $\mathcal{V}$  must satisfy the *optional ignorance* condition. Given these inputs, we can compute different estimates for  $\mathcal{V}$ -information, which is crucial to identify and interpret disparities in datasets. We categorize the corresponding estimations in three types of analyses: (1) dataset-level, (2) slicing, and (3) instance-level.

**Dataset-level:** first we assess whether  $X$ , which is used to predict  $Y$ , contains a significant amount of  $\mathcal{V}$ -information for predicting the variable  $S$ . If it does, models in  $\mathcal{V}$  are prone to produce biased outcomes. Consequently, the first metric to estimate is  $I_{\mathcal{V}}(X \mapsto S) = H_{\mathcal{V}}(S|\emptyset) - H_{\mathcal{V}}(S|X)$ . This proposed metric can generate insights through dataset-level comparisons. For example, given a dataset and several predictive families, this metric can issue warnings about the families that are likely to be more discriminatory. Similarly, given a predictive family and multiple datasets for the same task, the

metric can assist in identifying which dataset poses higher risks when used to learn a function from the family.

**Slicing:** the second assessment consists in finding the subsets of features that might potentially contribute to higher disparities. We call this goal slicing analysis. To this end, we build on the work of [Hewitt *et al.*, 2021], whose purpose is to capture the reduction in predictability when a certain subset of input features is known already. From [Hewitt *et al.*, 2021], let's assume the input space is partitioned into two subsets: a *known* subset  $C$  and an *unknown* subset  $\bar{C}$ , where features in  $\bar{C}$  are replaced by a constant value  $\bar{a}$ . [Hewitt *et al.*, 2021] formulate *conditional  $\mathcal{V}$ -information* as follows:

**Definition 6** (Conditional  $\mathcal{V}$ -information). *Given a predictive family  $\mathcal{V} \subseteq \Omega$ , the predictive  $\mathcal{V}$ -information from  $X_l$  to  $Y$  conditioned on the prior knowledge of  $C \subset \{X_1, \dots, X_n\} = X$  is defined as:*

$$I_{\mathcal{V}}(X_l \mapsto Y|C) = H_{\mathcal{V}}(Y|C) - H_{\mathcal{V}}(Y|C \cup X_l)$$

where  $\mathcal{V}$ -entropy  $H_{\mathcal{V}}(\cdot| \cdot)$  is now defined as:

$$H_{\mathcal{V}}(Y|C) = \inf_{f \in \mathcal{V}} \mathbb{E}_{c,y} [-\log f(c, \bar{a})[y]]$$

with  $c \in C$  and  $\bar{a} \in \bar{C}$ .

We propose to estimate the conditional  $\mathcal{V}$ -information for predicting the sensitive attribute and the target variable, given a specific feature  $X_l$ . This is represented as  $I_{\mathcal{V}}(X_l \mapsto T) = H_{\mathcal{V}}(T|\emptyset) - H_{\mathcal{V}}(T|X_l)$ , where  $T$  is set to either  $S$  or  $Y$ . We also propose to measure the amount of  $\mathcal{V}$ -information provided by variable  $l$ , information otherwise not present in the input space when  $X_l$  is excluded. To this end, we define  $C_{-l} = \{X_1, \dots, X_n\} \setminus X_l$ , where  $l \in \{1, \dots, n\}$ . The wanted conditional  $\mathcal{V}$ -information is then given by:  $I_{\mathcal{V}}(X \mapsto T|C_{-l}) = H_{\mathcal{V}}(T|C_{-l}) - H_{\mathcal{V}}(T|X)$ .

The fundamental intuition behind the proposed estimations is to determine whether, for a given ML pipeline, we are in an ideal low-risk scenario concerning the variable  $X_l$ . This scenario is characterized by high  $\mathcal{V}$ -information values for predicting the sensitive attribute  $S$ , and low values for the prediction of the target variable  $Y$ . This scenario is desirable because slicing out  $X_l$  from the input space would not compromise the useful information needed to predict  $Y$ . Any other scenarios would indicate a risk of disparities. For instance, a scenario with high values for both  $I_{\mathcal{V}}(X_l \mapsto S)$  and  $I_{\mathcal{V}}(X_l \mapsto Y)$ , but low values for  $\mathcal{V}$ -information when conditioned on  $C_{-l}$ , implies a significant risk of disparity. In fact, in this case  $X_l$  likely leaks usable information about  $S$ ; as such, outcomes can result in disparate predictions, and the removal of  $X_l$  cannot solve the problem since its  $\mathcal{V}$ -information is already encompassed within the other features. In this scenario, the dataset presents a high level of risk and poses substantial challenges for the implementation of mitigation approaches.

**Instance-level:** here, we aim to identify subsets of instances that are potentially at risk of being discriminated. We build on the work of [Ethayarajh *et al.*, 2022], which introduces the pointwise  $\mathcal{V}$ -information metric to estimate the degree of *usable information* in individual instances. This metric is defined as the difference in log-likelihood predictions of

the variable to be predicted (in this case, we assume  $s$ ) when no side information  $\emptyset$  is given, and when side information  $x$  is provided:

**Definition 7** (Pointwise  $\mathcal{V}$ -information (PVI)). *Given random variables  $X$  and  $S$ , and a predictive family  $\mathcal{V}$ , the pointwise  $\mathcal{V}$ -information (PVI) of  $(x, s)$  is*

$$PVI(x \mapsto s) = -\log f'[\emptyset](s) + \log f[x](s)$$

where  $f' \in \mathcal{V}$  s.t.  $\mathbb{E}[-\log f'[\emptyset](Y)] = H_{\mathcal{V}}(Y)$  and  $f \in \mathcal{V}$  s.t.  $\mathbb{E}[-\log f[X](Y)] = H_{\mathcal{V}}(Y|X)$ .

Unlike  $\mathcal{V}$ -information, PVI can be negative. Intuitively,  $PVI < 0$  implies that  $f \in \mathcal{V}$  is better at predicting  $s$  when  $\emptyset$  is given, rather than  $x$  (i.e., by outputting the majority class). This can occur due to various factors, such as mislabeling [Ethayarajh *et al.*, 2022], or an intrinsic error due to the underlying uncertainty in the ground truth.

For instance-level analysis, we propose estimating  $PVI_{\mathcal{V}}(x \mapsto s)$  where negative values suggest that models in  $\mathcal{V}$  are more accurate at predicting sensitive attributes by simply guessing the majority class rather than using the side information  $x$ . Conversely, positive values indicate that the models are better off using the side information to predict  $s$ . From a fairness perspective, both cases are problematic: when the model guesses the sensitive attribute to predict  $y$ , it may exacerbate disparities for underrepresented groups, and if a model can accurately predict  $s$  using information in  $x$ , it may be inadvertently identifying a feature highly correlated to the sensitive attribute, or it may reconstruct it. In contrast, a  $PVI_{\mathcal{V}}$  around 0 indicates less disparity risks, making it the preferable case.

## 4 Experimental Results

### 4.1 Datasets

We evaluated **DispaRisk** on four tabular and an image fairness benchmarks.

**Census Income (CI):** CI has 48,844 individuals with 14 features [Dheeru and Taniskidou, 2017]. The sensitive attribute is gender. The target variable encodes whether the income is greater than 50K [Asuncion and Newman, 2007].

**Dutch Census (DC):** this dataset has 60,420 observations of Dutch individuals from 1973-1975 [Le Quy *et al.*, 2022] with 12 features, such as age and education. The sensitive attribute is sex and the binary target is the occupation feature with *high income level* and *low income level* classes.

**Compas Recidivism (CR):** this dataset has 7,214 observations of individuals in the criminal justice system with features on felonies, misdemeanors, charges, age, sex, race and jailed days. Race is the sensitive attribute, describing whether an individual is African-American or not. The target variable encodes whether the individual re-offended in two years [ProPublica, 2016].

**Credit Card (CC):** this dataset has 30,000 observations of Taiwanese customers' default payments in October 2005 with 24 features [Le Quy *et al.*, 2022]. We use sex as sensitive attribute and as target variable whether customer faces a default situation in the following month.

**CelebFaces Attribute (CelebA):** This dataset includes over 200,000 face images of celebrities. The source provides also

39 binary attributes and 5 landmarks that specify the pixel location of five facial features [Liu *et al.*, 2015]. Following Zhang *et al* [Zhang *et al.*, 2022], gender is the sensitive attribute and the binary variable *BlondHair* is the target.

For the each dataset, we use the train/test partitions given by the source of the data. If no partitions are given, we randomly split the dataset using a 70/30 ratio for training and test sets. The training sets are used to fine-tune the predictive families and the test sets are used to estimate the  $\mathcal{V}$ -information measures. During training, we estimate performances under cross-validation and one held-out validation set strategies in tabular and CelebA datasets, respectively. In addition, we apply label encoding to categorical variables and scale all features by subtracting the mean and normalizing into unit variance. For the CelebA dataset, following Zhang *et al* [Zhang *et al.*, 2022], the images are resized, cropped and flipped.

### 4.2 Predictive Families and Estimates

We explore five predictive families. The first family consists of linear classifier models followed by the sigmoid function  $\sigma$ ; we call this family *Linear* and set  $w$  and  $b$  its parameters. The next three families consist of nested affine function classifiers with ReLU as activation function and a sigmoid at the top. We construct the three families with Multi-Layer Perceptrons (MLP) function, denoting with 1MLP, 2MLP, and 3MLP the one-layer, two-layers, and 3-layers MLP, respectively. We also use  $m_i$  to denote the perceptron function, where  $i$  indicates the number of layers. The last two families are used only for the CelebA dataset, and consist of convolutional neural networks (CNNs), followed by fully connected layers and a softmax output layer. We follow ResNet18 (RN) [He *et al.*, 2016] and AlexNet (AN) [Krizhevsky *et al.*, 2017] architectures to construct two families of CNNs:

$$\begin{aligned} \mathcal{V}_{Linear} &= \{h : X \mapsto f[x](y) = \sigma(-w[x] + b)\} \\ \mathcal{V}_{1MLP} &= \{h : X \mapsto f[x](y) = \sigma(m_1(x))\} \\ \mathcal{V}_{2MLP} &= \{h : X \mapsto f[x](y) = \sigma(m_2(x))\} \\ \mathcal{V}_{3MLP} &= \{h : X \mapsto f[x](y) = \sigma(m_3(x))\} \\ \mathcal{V}_{RN} &= \{h : X \cup S \mapsto RN(x)\} \\ \mathcal{V}_{AN} &= \{h : X \cup S \mapsto AN(x)\} \end{aligned}$$

The estimate of  $\mathcal{V}$ -information involves fitting models to the training set by minimizing the negative log-loss. We establish two early-stop criterion: a tolerance of  $1 - e4$  to prevent over-fitting and a max number of epochs equal to 1000. The loss is computed on a validation set, of size 10% of train set, at each epoch. If the improvement in loss does not exceed the set tolerance value in ten consecutive epochs or the max number of epochs is reached, the training is halted. The model exhibiting the minimal loss on the validation set is used for further analysis. For  $\mathcal{V}_{Linear}$  we apply the  $L_1$  and  $L_2$ -norm penalty, and for the MLP families we experiment with layer sizes of 10, 100, and 500. For each training, we use the Adam optimizer with a learning rates in  $\{1e - 5, 1e - 4, 1e - 3, 1e - 2, 1e - 1, 1.0\}$ ,  $\beta_1 = 0.9$  and  $\beta_2 = 0.99$ , and batch size of 512. To ensure that our results are robust to model selection and initialization, we train multiple models with different hyperparameters and seeds, and

Table 1:  $I_{\mathcal{V}}(X \mapsto S)$  (abbreviated as  $I_{\mathcal{V}}(S)$ ), Demographic Parity, and Accuracy on predicting  $Y$  for each  $\mathcal{V}$  across tabular datasets. Reported values are computed as the mean of the top 25% performing models. The  $I_{\mathcal{V}}(X \mapsto S)$ , metric helps identify predictive families with higher unfairness concerns on a given dataset. Bold font indicates highest values.

$\mathcal{V}$ -family	Census Income			Dutch Census			Compas Recidivism			Credit Card		
	$I_{\mathcal{V}}(S)$	$\Delta_{DP}$	acc									
Linear	.185	.132	.820	.060	.186	.805	.042	.199	.688	.010	.017	.811
1MLP	<b>.317</b>	<b>.176</b>	<b>.851</b>	.099	<b>.196</b>	.821	<b>.046</b>	.211	<b>.692</b>	.024	<b>.020</b>	<b>.819</b>
2MLP	.313	.169	<b>.851</b>	.099	.192	<b>.822</b>	.046	.215	.690	.022	.018	<b>.819</b>
3MLP	.310	.168	<b>.851</b>	<b>.103</b>	.193	<b>.822</b>	<b>.046</b>	<b>.220</b>	<b>.692</b>	<b>.025</b>	.018	<b>.819</b>

**Algorithm 1** Predictive  $\mathcal{V}$ -information and pointwise  $\mathcal{V}$ -information estimates

**Input:**  $\mathcal{D}_{train} = \{(x_i, t_i)\}_{i=1}^k$ ,  $\mathcal{D}_{test} = \{(x_i, t_i)\}_{i=1}^m$  with  $k + m = n$  and  $t_i$  as the target label of the point  $i$ , family  $\mathcal{V}$  and subset  $C \subseteq X$ , subset  $\bar{C}$  with  $\bar{C} \cap C = \emptyset$

**Output:**  $\hat{I}_{\mathcal{V}}$  and PVI estimates.

**do**

```

 $g \leftarrow$  fine-tune  $\mathcal{V}$  on  $\mathcal{D}_{train}$ 
 $g' \leftarrow$  fine-tune  $\mathcal{V}$  on  $\mathcal{D}_{train}$  with partition  $C, \bar{C}$ 
 $H_{\mathcal{V}}(T|X) \leftarrow 0$ 
 $H_{\mathcal{V}}(T|C) \leftarrow 0$ 
for  $(x_i, t_i) \in \mathcal{D}_{test}$  do
     $H_{\mathcal{V}}(T|X) \leftarrow H_{\mathcal{V}}(T|X) - \frac{1}{m} \log g[x_i](t_i)$ 
     $H_{\mathcal{V}}(T|C) \leftarrow H_{\mathcal{V}}(T|C) - \frac{1}{m} \log g'[c_i, \bar{c}_i](t_i)$ 
     $\text{PVI}(x_i \mapsto t_i) \leftarrow -\log g'[c_i, \bar{c}_i](t_i) + \log g[x_i](t_i)$ 
end for
 $\hat{I}_{\mathcal{V}}(X \mapsto T|C) = H_{\mathcal{V}}(T|C) - H_{\mathcal{V}}(T|X)$ 
end do
```

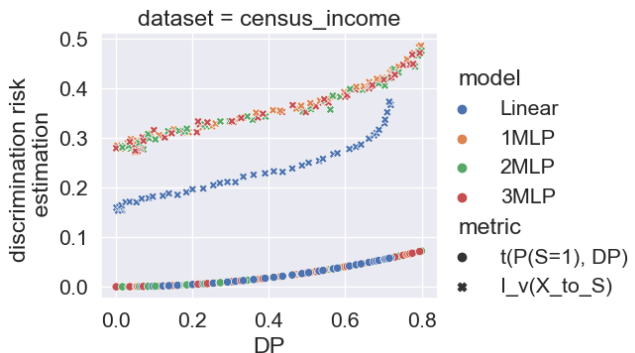


Figure 1:  $t(P(S = 1), \Delta_{DP})$  and  $I_{\mathcal{V}}(X \mapsto S)$  estimates in CI datasets from samplings datasets such that  $P(S = 1) = k$  with  $k \in \{0.05, 0.07, \dots, 0.95\}$ , leading to different levels of  $\Delta_{DP}$  of models trained on them.

select the one with the minimal loss function for downstream fairness analysis.

Once the models have been trained, we estimate the  $\mathcal{V}$ -entropy, the  $\mathcal{V}$ -information, and the PVI on the test set by using Algorithm 1. This has computational complexity of  $O(n)$ . Then, we set  $T$  and the partitions  $C, \bar{C}$  accordingly. In the algorithm,  $T$  denotes the variable to be predicted and can be the target or the sensitive attribute. For instance, to estimate  $I_{\mathcal{V}}(X \mapsto S)$ , we set  $T = S$  and the subset

$C = \emptyset$ ; for  $I_{\mathcal{V}}(X_l \mapsto Y|C_{-l})$ , we set  $T = Y$  and the subset  $C = C_{-l} = \{X_1, \dots, X_d\} \setminus X_l$ . Additionally, we use  $\ln$ , hence estimates are in natural unit of information. The estimate procedure assumes a large dataset size [Xu *et al.*, 2020]. For each dataset, we found that after using about 90% of the training data, the estimates reach a plateau. More details are in the supplementary material. Finally, experiments were run with 4x NVIDIA A100-SXM-80GB GPU and 2x AMD MILAN, taking 62.97 minutes on average for fine-tuning in the largest dataset (CelebA).

### 4.3 Analysis.

In this section we present major findings grouped in four research questions (RQ). More results that support our conclusions are available in the supplementary material.

**RQ1: Can we use predictive  $\mathcal{V}$ -information to measure the disparities induced by the dataset in downstream ML models?** We generate multiple trials of each tabular dataset by resampling the majority group with replacement, representing different sample collection methods. For each trial, we estimate  $I_{\mathcal{V}}(X \mapsto S)$  and  $\Delta_{DP}$ , and depict the results in Figure 1 for CI dataset. See Supplementary material for the rest datasets. From the figure, higher disparities clearly correlate with higher predictive  $\mathcal{V}$ -information, supporting the intuition developed in Section 2.2. Hence, stakeholders can rely on *usable information* for early identification of disparity risks in datasets within the context of a ML pipeline.

**RQ2: Which predictive families tend to produce higher levels of disparities when measured with standard fairness metrics for a given dataset?** Tables 1 and 2 present the accuracy and demographic parity of models, and the estimates following the dataset-level analysis. From the tables, we observe a strong correlation between  $I_{\mathcal{V}}(X \mapsto S)$  and  $\Delta_{DP}$ . Furthermore, we find that models with higher  $\mathcal{V}$ -information tend to be more accurate. This emphasizes disparity risks, as these models are more likely to be finally deployed. Therefore, **DispaRisk** provides early information to stakeholders about the potential challenge of balancing performance and fairness.

**RQ3: Which features contribute more to disparities?** To answer this question, we follow the slicing analysis of **DispaRisk**. First, we select the family with higher accuracy to estimate the  $\mathcal{V}$ -information of each feature  $X_l$  to predict the sensitive attribute  $S$  and the target  $Y$ . We report here the results on the CR dataset with  $\mathcal{V}_{1MLP}$ ; results for the remaining tabular datasets are included in the Supplementary Material. Table 3 shows the estimates when using only fea-

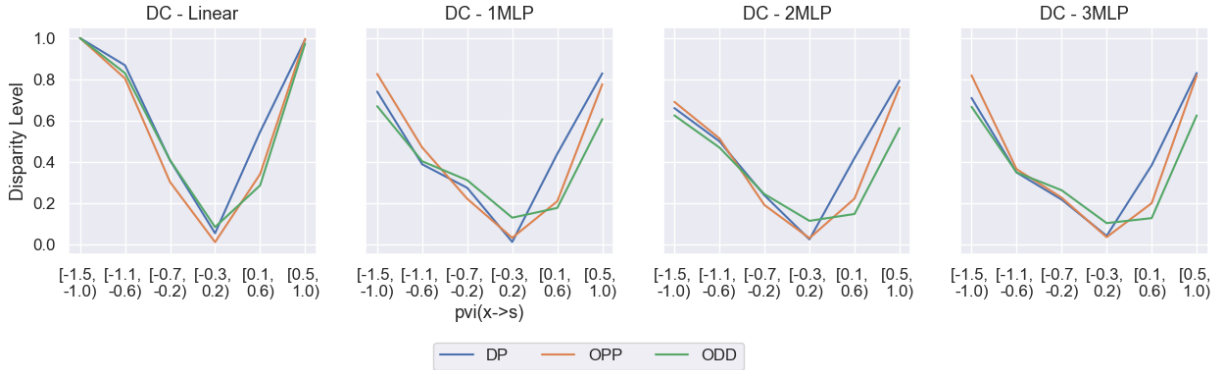


Figure 2: Fairness metrics for sorted 0.5-PVI-size-bins of DC, ranging from  $-1.5$  to  $1.1$ , with steps of  $0.3$ .

Table 2:  $I_V(X \mapsto S)$ , Demographic Parity, and Accuracy on predicting  $Y$  reported for each  $V$  across tabular datasets. The  $I_V(X \mapsto S)$  metric helps identify predictive families with higher unfairness concerns on a given dataset. Bold font indicates highest values.

$V$ -family	CelebA		
	$I_V(X \mapsto S)$	$\Delta_{DP}$	acc
Linear	.222	.103	.899
1MLP	.358	.148	.934
2MLP	.360	.156	.936
3MLP	.367	.153	.936
RN	<b>.620</b>	<b>.191</b>	<b>.960</b>
AN	.606	.186	.959

Table 3: Predictive  $V$ -information for  $S$  and  $Y$  from  $X_l$  in CR, given  $V_{1MLP}$ . Values are sorted by  $I_V(X_l \mapsto S)$  and shown in nats of information.

Feature	$I_V(X_l \mapsto S)$	$I_V(X_l \mapsto Y)$
priors_count	<b>.026</b>	<b>.061</b>
age	<b>.010</b>	<b>.019</b>
age_cat	<b>.008</b>	<b>.013</b>
juv_misd_count	.007	.010
juv Fel_count	.005	.007
c_charge_degree	.003	.006
juv_other_count	.002	.009
c_days_jail	.001	.001
sex	< .001	.004

Table 4: Conditional  $V$ -information for predicting  $S$  and  $Y$  from  $X_l$  in the CR, given  $V_{1MLP}$ . Values are sorted by  $I_V(X \mapsto S|C_{-l})$  and shown in nats of information.

Feature	$I_V(X \mapsto S C_{-l})$	$I_V(X \mapsto Y C_{-l})$
priors_count	<b>.024</b>	<b>.061</b>
age_cat	<b>.001</b>	.001
age	<b>.001</b>	<b>.010</b>
c_charge_degree	< .001	< .001
c_days_jail	< .001	<b>.002</b>
sex	< .001	.002
juv_misd_count	< .001	< .001
juv Fel_count	< .001	< .001
juv_other_count	< .001	.002

ture  $X_l$ , while Table 4 depicts the  $V$ -information when using all features except  $X_l$ . In each table, the results are sorted by predictive information with respect to  $S$ . From Table 3, it is evident that “previous criminal history” (`priors_count`) and “age” have the strongest *usable* signals for  $V_{1MLP}$  in predicting whether the defendant will re-offend within two years. However, providing these features as side information might increase the risk of disparities since they also have the highest *usable information* in relationship to race, the sensitive attribute. This increment depends on which proportion of their predictive information is already in the input space, with lower values about  $S$  and higher levels about  $Y$  being preferable. Then, we re-estimate the  $V$ -information conditioned on  $C_{-l}$ , and the results are shown in Table 4. From the table, “previous criminal history” and “age” have the highest conditional predictive information for both  $S$  and  $Y$ . This means that removing them from the input space can improve fairness, but will reduce the predicting power of the target variable for  $V_{1MLP}$ , while using them poses a risk. Overall, the derived risk-information can be given to stakeholders, who can then pursue an informed and non-trivial pre-processing and mitigating approaches, focused on the involved variables.

We apply the same analysis on the CelebA dataset using AN. We assume that the provided five landmarks are the features of interest for analysis. Additionally, we introduce a sixth feature called *bottom-right* which represents a less biased feature, i.e., it has a lower amount of predictive information about gender. To capture the information from these features, we select a square region (with a 10, 20, or 40-pixel sizes) centered at the landmarks, and mask with a value of 1.0 the pixels within or outside the square, depending on the desired estimate. Table 5 presents the estimated  $V_{AN}$ -information for each feature in predicting sensitive and target variables. We observe that varying the mask size results in an increase in predictive information; larger mask sizes provide the models with more *usable information*, thereby enhancing their possible predictive capabilities. Moreover, we notice a substantial amount of predictive information contained in the “eyes” feature for  $V_{AN}$ , enabling accurate predictions of both the sensitive (gender) and the target variable (`BlondHair`). However, as discussed previously, this presents an undesirable scenario. The removal of “eyes” features eliminates a

Table 5: The  $\mathcal{V}_{AN}$ -information of features in the CelebA dataset. We use the landmarks provided in the source. We also use square masks of different sizes, 10, 20, and 40 pixels, and combined features. Specifically, eyes: left\_eye+right\_eye; mouth: left\_mouth+right\_mouth; and all: eyes+mouth+nose. Additionally, we add a less biased features positioned in the bottom-right corner of the pictures. We group the features in two groups: single (top) and mixed (bottom), and apply bold font to the two highest estimates for a given size of mask.

Feature	$I_{\mathcal{V}}(X_l \mapsto S)$			$I_{\mathcal{V}}(X_l \mapsto Y)$			$I_{\mathcal{V}}(X \mapsto S C_{-l})$			$I_{\mathcal{V}}(X \mapsto Y C_{-l})$		
	10p	20p	40p	10p	20p	40p	10p	20p	40p	10p	20p	40p
left_eye	<b>.288</b>	<b>.453</b>	<b>.526</b>	.032	<b>.083</b>	<b>.171</b>	.004	.003	<b>.041</b>	.002	.002	<b>.005</b>
right_eye	<b>.297</b>	<b>.460</b>	<b>.529</b>	<b>.034</b>	<b>.081</b>	<b>.158</b>	<b>.006</b>	<b>.006</b>	<b>.050</b>	<b>.003</b>	<b>.003</b>	<b>.009</b>
left_mouth	.190	.334	.458	.018	.035	.097	.005	.003	.020	.001	<b>.003</b>	.003
right_mouth	.189	.335	.466	.020	.035	.080	.005	.001	.013	.001	.002	.003
nose	.086	.249	.471	.010	.033	.053	<b>.006</b>	<b>.014</b>	.025	<b>.002</b>	<b>.003</b>	.004
bottom_right	.061	.105	.167	<b>.035</b>	.066	.109	.001	.002	.001	.002	.001	.002
eyes	.360	.509	.567	.042	.098	.208	<b>.170</b>	.173	<b>.184</b>	.014	.016	.032
mouth	.264	.423	.526	.023	.046	.128	.017	.026	.045	.002	.005	.013
eyes+nose	<b>.413</b>	<b>.536</b>	<b>.585</b>	<b>.046</b>	<b>.107</b>	<b>.211</b>	.137	<b>.254</b>	.141	<b>.015</b>	<b>.027</b>	<b>.042</b>
mouth+nose	.326	.464	.549	.033	.053	.134	.023	.032	.064	.006	.006	.012
all	<b>.475</b>	<b>.562</b>	<b>.596</b>	<b>.059</b>	<b>.111</b>	<b>.216</b>	<b>.234</b>	<b>.326</b>	<b>.197</b>	<b>.025</b>	<b>.028</b>	<b>.069</b>

relevant amount of *usable information* pertaining to the gender, but this comes at the expense of losing significant information about “hair color”. This shows that mitigating disparity in CelebA datasets, such as learning a fair representation, is challenging for the  $\mathcal{V}_{AN}$  predictive family.

**RQ4: Which individuals are at a higher risk of being discriminated against?** Following **DispaRisk**’s Instance-level analysis, we estimated  $\text{PVI}_{\mathcal{V}}(x \mapsto s)$  for each individual, sorted the estimated values, and grouped them into  $p$ -sized discretized bins starting at  $-1.5$  and finishing at  $1.1$  with steps of  $t \leq p$ . We then calculated  $\Delta_{DP}$ ,  $\Delta_{ODD}$ , and  $\Delta_{OPP}$  for each bin. The objective is to demonstrate the claim made in Section 3 that individuals with  $\text{PVI}$  closer to 0 are less likely to face discrimination. Figure 2 depicts results for the DC dataset. See the supplementary material for the remaining datasets.

From the figures, the individual bins with  $\text{PVI}$  closer to  $-1.5$  or  $1.1$  exhibit the higher disparities, while those closer to 0 show the lower levels of unfairness. This suggests that finding a proper representation where  $\text{PVI}$ s are reduced to 0 is promising for mitigating disparities in the downstream pipeline. Moreover, tailoring the representation to the predictive family rather than creating a general representation for every model may be advantageous in this regard.

Finally, we can also find individuals profiles with high risks of discrimination by using their  $\text{PVI}$ s estimates. Figure 3 shows the mean of “previous criminal history” and “age” in the CR dataset of each bins of  $\text{PVI}$  estimates. From the figure, when guessing (negative  $\text{PVI}$ ) or using side information (positive  $\text{PVI}$ ), we observe a larger difference between demographic groups. In particular, older individuals with more prior felonies are likely to face discrimination from the  $\mathcal{V}_{MLP}$  family models.

## 5 Conclusions

We introduced **DispaRisk**, a framework that provides insights into disparity risks for downstream workflows. Data owners can use **DispaRisk** to choose proper *pre-processing* mitigation approaches to reduce disparity risks. **DispaRisk** also

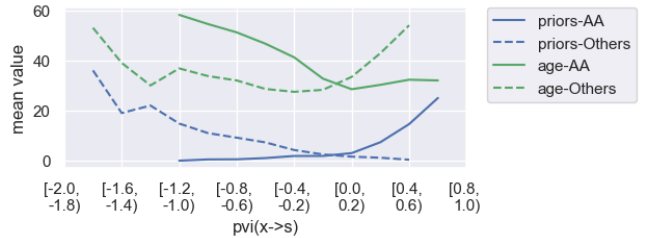


Figure 3: `priors_count` and `age` averages for each demographic group sorted by  $\text{PVI}$ .

guides feature-level and instance-level analysis at early stages of a ML pipeline. Our experiments showcase that the estimates from **DispaRisk** have the following desirable properties: (1) they correlate with disparities, enabling early identification of discrimination risks; (2) facilitate the identification of risky families, eliminating the need to recompute *post-processing* metrics dependent on and specific for pre-trained models; (3) provide explainability insights about which features may increase risks due to the substantial information of sensitive attribute, and allow for flagging challenging datasets for fairness mitigation tasks; and (4) enable the identification of individual profiles in the dataset at high risk. Furthermore, auditing datasets by using *usable information* showed virtues in our experiments, compared to another approach of using metrics computed directly from a given trained model (a more post-processing approach): **DispaRisk**’s approach aims to estimate risk from a more generalizable perspective based on ML pipeline computational capabilities, making the risk estimations specific to the pipeline rather than an instance of the it defined by the models already trained. Nevertheless, although our experiments show promising results, they are limited to binary sensitive attribute and classification tasks. **DispaRisk** is extendible to these settings, thus we plan to explore them in future research. Additionally, we also plan to explore **DispaRisk** in other machine learning domains, such as unsupervised learning and Natural Language Processing.

## References

[Asuncion and Newman, 2007] Arthur Asuncion and David Newman. Uci machine learning repository, 2007.

[Chen *et al.*, 2023] Richard J Chen, Judy J Wang, Drew FK Williamson, Tiffany Y Chen, Jana Lipkova, Ming Y Lu, Sharifa Sahai, and Faisal Mahmood. Algorithmic fairness in artificial intelligence for medicine and healthcare. *Nature Biomedical Engineering*, 7(6):719–742, 2023.

[Cover and Thomas, 2006] M Thomas Cover and A Joy Thomas. *Elements of Information Theory*. Wiley-Interscience, 2006.

[Dheeru and Taniskidou, 2017] Dua Dheeru and E Karra Taniskidou. Uci machine learning repository. 2017.

[Ethayarajh *et al.*, 2022] Kawin Ethayarajh, Yejin Choi, and Swabha Swamyamdipta. Understanding dataset difficulty with  $\mathcal{V}$ -usable information. In *International Conference on Machine Learning*, pages 5988–6008. PMLR, 2022.

[Feldman *et al.*, 2015] Michael Feldman, Sorelle A. Friedler, John Moeller, Carlos Scheidegger, and Suresh Venkatasubramanian. Certifying and removing disparate impact. In *Proceedings of the 21th ACM SIGKDD International Conference on Knowledge Discovery and Data Mining*, KDD ’15, page 259–268, New York, NY, USA, 2015. Association for Computing Machinery.

[Fu *et al.*, 2021] Runshan Fu, Yan Huang, and Param Vir Singh. Crowds, lending, machine, and bias. *Information Systems Research*, 32(1):72–92, 2021.

[Gitiaux and Rangwala, 2021] Xavier Gitiaux and Huzefa Rangwala. Learning smooth and fair representations. In Arindam Banerjee and Kenji Fukumizu, editors, *Proceedings of The 24th International Conference on Artificial Intelligence and Statistics*, volume 130 of *Proceedings of Machine Learning Research*, pages 253–261. PMLR, 13–15 Apr 2021.

[Gitiaux and Rangwala, 2022] Xavier Gitiaux and Huzefa Rangwala. Sofair: Single shot fair representation learning. *arXiv preprint arXiv:2204.12556*, 2022.

[Gupta *et al.*, 2021] Umang Gupta, Aaron M Ferber, Bistra Dilkina, and Greg Ver Steeg. Controllable guarantees for fair outcomes via contrastive information estimation. In *Proceedings of the AAAI Conference on Artificial Intelligence*, volume 35, pages 7610–7619, 2021.

[Hardt *et al.*, 2016] Moritz Hardt, Eric Price, Eric Price, and Nati Srebro. Equality of opportunity in supervised learning. In D. Lee, M. Sugiyama, U. Luxburg, I. Guyon, and R. Garnett, editors, *Advances in Neural Information Processing Systems*, volume 29. Curran Associates, Inc., 2016.

[Hardt *et al.*, 2021] Michaela Hardt, Xiaoguang Chen, Xiaoyi Cheng, Michele Donini, Jason Gelman, Satish Gollaprolu, John He, Pedro Larroy, Xinyu Liu, Nick McCarthy, et al. Amazon sagemaker clarify: Machine learning bias detection and explainability in the cloud. In *Proceedings of the 27th ACM SIGKDD Conference on Knowledge Discovery & Data Mining*, pages 2974–2983, 2021.

[He *et al.*, 2016] Kaiming He, Xiangyu Zhang, Shaoqing Ren, and Jian Sun. Deep residual learning for image recognition. In *Proceedings of the IEEE Conference on Computer Vision and Pattern Recognition (CVPR)*, June 2016.

[Hewitt *et al.*, 2021] John Hewitt, Kawin Ethayarajh, Percy Liang, and Christopher Manning. Conditional probing: measuring usable information beyond a baseline. In *Proceedings of the 2021 Conference on Empirical Methods in Natural Language Processing*, pages 1626–1639, Online and Punta Cana, Dominican Republic, November 2021. Association for Computational Linguistics.

[Kizilcec and Lee, 2022] René F Kizilcec and Hansol Lee. Algorithmic fairness in education. In Wayne Holmes and Kaška Porayska-Pomsta, editors, *The Ethics of Artificial Intelligence in Education*, pages 174–202. Taylor & Francis, 2022.

[Krizhevsky *et al.*, 2017] Alex Krizhevsky, Ilya Sutskever, and Geoffrey E Hinton. Imagenet classification with deep convolutional neural networks. *Communications of the ACM*, 60(6):84–90, 2017.

[Le Quy *et al.*, 2022] Tai Le Quy, Arjun Roy, Vasileios Iosifidis, Wenbin Zhang, and Eirini Ntoutsi. A survey on datasets for fairness-aware machine learning. *Wiley Interdisciplinary Reviews: Data Mining and Knowledge Discovery*, page e1452, 2022.

[Liu *et al.*, 2015] Ziwei Liu, Ping Luo, Xiaogang Wang, and Xiaou Tang. Deep learning face attributes in the wild. In *Proceedings of International Conference on Computer Vision (ICCV)*, December 2015.

[Pessach and Shmueli, 2023] Dana Pessach and Erez Shmueli. *Algorithmic Fairness*, pages 867–886. Springer International Publishing, Cham, 2023.

[ProPublica, 2016] ProPublica. How we analyzed the compas recidivism algorithm. *ProPublica*, 2016.

[Vasquez *et al.*, 2022] Jonathan Vasquez, Xavier Gitiaux, Cesar Ortega, and Huzefa Rangwala. Faired: A systematic fairness analysis approach applied in a higher educational context. In *LAK22: 12th International Learning Analytics and Knowledge Conference*, pages 271–281, 2022.

[Wen *et al.*, 2021] Min Wen, Osbert Bastani, and Ufuk Topcu. Algorithms for fairness in sequential decision making. In *International Conference on Artificial Intelligence and Statistics*, pages 1144–1152. PMLR, 2021.

[Xu *et al.*, 2020] Yilun Xu, Shengjia Zhao, Jiaming Song, Russell Stewart, and Stefano Ermon. A theory of usable information under computational constraints. In *International Conference on Learning Representations (ICLR)*, 2020.

[Zhang *et al.*, 2022] Guanhua Zhang, Yihua Zhang, Yang Zhang, Wenqi Fan, Qing Li, Sijia Liu, and Shiyu Chang. Fairness reprogramming. In *Thirty-sixth Conference on Neural Information Processing Systems*, 2022.